Effects of temperature on physicochemical properties of the lecithin-based deep eutectic solvents and their use in the CaO-catalyzed transesterification

Zoran B. Todorović[1], Biljana S. Đordević[1], Dragan Z. Troter[1], Ljiljana M. Veselinović[2], Miodrag V. Zdujić[2] and Vlada B. Veljković[1,3]

[1]*University of Niš, Faculty of Technology, Bulevar Oslobođenja 124, 16000 Leskovac, Serbia*
[2]*Institute of Technical Sciences of the Serbian Academy of Sciences and Arts, Knez Mihailova 35, 11000 Belgrade, Serbia*
[3]*Serbian Academy of Sciences and Arts, Knez Mihailova 35, 11000 Belgrade, Serbia*

Abstract

Deep eutectic solvents (DESs) are called 'designer solvents' due to various structural variations and the benefit of tailoring their physicochemical properties. For industrial applications of DESs it is crucial to know their physical and thermodynamic properties such as density, viscosity, and refractive index. These properties were measured for three lecithin (LEC)-based DESs with glycerol (G), triethanolamine (TEOA), and oleic acid (OLA) as functions of temperature. The viscosity was fitted by both Arrhenius-type and Vogel-Tamman-Fulcher equations. The density, viscosity, and refractive index of tested DESs decreased with the increase in temperature. The LEC:G DES exhibited the lowest density at all tested temperatures. This DES was selected as a cosolvent in the ethanolysis of cold-pressed black mustard (*Brassica nigra* L.) seed oil catalyzed by either calcined or non-calcined CaO. The reaction was carried out in a batch stirred reactor under the following conditions: the temperature of 70 °C, the ethanol-to-oil molar ratio of 12:1, and the amount of DES and CaO of 20 and 10 wt.% (to oil), respectively. The presence of DES accelerated the reaction, while the separation of the final reaction mixture phases was faster.

Keywords: Brassica nigra L.; black mustard; ethanolysis; fatty acid ethyl esters; deep eutectic solvent.

Available on-line at the Journal web address: http://www.ache.org.rs/HI/

ORIGINAL SCIENTIFIC PAPER

UDC: 615.015.14:66.094.942:(544.344.015.33+ 544.351-145.82)

Hem. Ind. **77(1)** 53-67 (2023)

1. INTRODUCTION

Tendency to eliminate or reduce the use of organic solvents in various technological processes has led to the increased interest in developing different 'green' solvents, such as deep eutectic solvents (DESs). DESs are defined as mixtures of two or more components, hydrogen bond acceptors (usually choline chloride (ChCl)) and hydrogen bond donors (like alcohols, amides, carboxylic acids, esters, ethers, etc.), which are interconnected by hydrogen bonds. This newly formed mixture has a melting point lower than the individual components. These solvents are desirable and acceptable due to the possibility of adjusting their properties by selecting the appropriate components (often natural, cheap, safe, and available) that enable the formation of hydrogen bonds. Appropriate DESs possess several advantages: low cost, easy preparation, biodegradability, nontoxicity, wide liquid range, non-volatility, thermal stability, and non-reactivity with water [1]. However, for applying any DES, for instance, in biodiesel production combined with non-edible vegetable oils, it is essential to determine their physical and thermodynamic properties.

In recent years, the application of DESs as efficient cosolvents or catalysts in biodiesel synthesis has been raising attention [2,3]. ChCl:glycerol (ChCl:G) DES has been successfully applied for transesterification of different oils, such as palm oil [3], expired sunflower oil [4], cooking waste oil [5], rapeseed oil [6], and *Xanthoceras sorbifolia* Bunge seed oil [7]. The

Corresponding authors: Vlada B. Veljković, Faculty of Technology, University of Niš, Bulevar Oslobođenja 124, 16000 Leskovac, Serbia
E-mail: veljkovicvb@yahoo.com
Paper received: 27 May 2022; Paper accepted: 17 September 2022; Paper published: 3 October 2022.
https://doi.org/10.2298/HEMIND220527016T

application of DESs for biodiesel production from black mustard (*Brassica nigra* L., Brassicaceae) seed oil (BMSO) has not been reported in the literature.

Black mustard is one of the few oilseeds adapted to colder regions, with a minimum amount of pesticides and other agricultural inputs [8]. BMSO contains a large proportion of erucic acid (up to 50 %) that can harm the cardiovascular system, so its application in the diet must be cautious [9]. However, due to containing single double-bond, branched, and long-chain fatty acids, this oil has lower pour and cloud points than the oils with a higher content of saturated fatty acids, making it suitable for diesel engines as an alternative fuel [10,11]. Biodiesel produced from BMSO demonstrates excellent potential as a lubricant additive with lower cloud and pour points (3.5 and -15 °C, respectively), making it suitable for regions with cold climates [8]. Shahzadi et al. [12] performed the KOH-catalyzed methanolysis of a previously esterified BMSO, while Aslan and Eryilmaz [10] reported the KOH-catalyzed ethanolysis of BMSO.

Since lecithin (LEC) has the same choline group in its structure as ChCl, it seems to be a possible replacement for ChCl, a well-known substance used for preparing various DESs. It represents a mixture of naturally occurring lipids, from which more than 50 % are phospholipids [13]. As a surfactant with a hydrophilic head and two hydrophobic tails, LEC forms organogels [14,15], which are used for preparation of cosmetic and pharmaceutical formulations [13], drug delivery [16], lubrication, food processing [17], and extraction [14,18]. The amphiphilic molecular structure of LEC also allows its application as a natural emulsifier in food products [17,19,20]. However, the use of LEC to prepare DESs is not reported in the literature.

In this paper, three novel DESs were prepared by combining LEC with G, triethanolamine (TEOA), or oleic acid (OLA) in a molar ratio of 1:2. Density, viscosity, and refractive index of these DESs were measured at atmospheric pressure in the temperature range of 293.15-363.15 K relevant for the practical use. Several thermodynamic properties were calculated, such as molar volume, lattice energy, heat capacity, as well as molar Gibbs energy, enthalpy, and entropy of activation of viscous flow. Finally, the possibility of using the LEC:G DES as a suitable replacement for the ChCl:G DES as a cosolvent in the heterogeneously-catalyzed ethanolysis of cold-pressed BMSO was tested in which either calcined or non-calcined CaO was used as catalysts. Moreover, the catalytic activities of non-calcined and calcined CaO without or with LEC:G or ChCl:G DESs were compared. To the best of the authors' knowledge, this is the first study of the physical and thermodynamic properties of the DESs mentioned above and the application of the LEC-based DES in transesterification reactions.

2. EXPERIMENTAL

2. 1. Materials

For the preparation of the DESs, soybean LEC (from TCI, Germany), G (Ph Eur grade, MeiLab, Belgrade, Serbia), OLA (99 %, Sigma-Aldrich, St. Louis, USA), and TEOA (99.%, Centrohem, Stara Pazova, Serbia) were used. CaO (extra pure) and ChCl (≥ 98.0 %) were obtained from Sigma Aldrich (St. Louis, USA). Absolute ethanol (99.5 %) was purchased from Sani-Hem (Novi Bečej, Serbia). HPLC grade methanol, 2-propanol, and *n*-hexane were provided from Lab-Scan (Dublin, Ireland). Ethyl acetate (99.5 %, Merck-Millipore, Darmstadt, Germany) and glacial acetic acid (Zorka, Šabac, Serbia) were employed as solvents. Hydrochloric acid (36.0 %) was purchased from Centrohem (Stara Pazova, Serbia). The standards of triolein, diolein, and monoolein and the standards containing ethyl esters of palmitic, stearic, oleic, linolenic, and linoleic acids (20.0 % of each ester), were provided from Sigma-Aldrich (St. Louis, USA).

2. 2. Cold pressing of black mustard seeds

Black mustard seeds were provided from the Institute of Field and Vegetable Crops, Novi Sad, Serbia. The moisture content of the seeds (4.2 ± 0.2 wt.%) was determined by drying seeds at 105 °C until constant weight. The BMSO was obtained by cold pressing (oil press Komet, Germany) and filtered first under vacuum through a sterile gauze and filter paper to remove all impurities. The physicochemical properties of the oil were as follows: the density of 985.1 kg m^{-3} at 20 °C, the viscosity of 123.3 mPa·s at 25 °C, the acid value of 2.08 mg KOH/g, the saponification value of 169.4 mg KOH / g, and the iodine value of 99.2 g I_2 / 100 g [9].

2. 3. Preparation of LEC-based DESs

LEC was mixed with the desired compound (G, TEOA, or OLA) at the molar ratio of 1:2 in a round-bottom flask. The flask was placed on a rotary evaporator at 348.15 K until a homogeneous viscous liquid was obtained, as described elsewhere [21]. The prepared DESs were stored in glass bottles placed in a desiccator with $CaCl_2$ until use.

2. 4. Measurements of the physical properties of LEC-based DESs

Density, viscosity, and refractive index were measured by using a densitometer (DMA 4500 Anton Paar, Austria), rotational viscometer (Visco Basic Plus, ver. 0.8, Fungilab S.A., Barcelona, Spain), and an automatic refractometer (Atago A100, Japan), respectively, at atmospheric pressure in the temperature range between 293.15 and 363.15 K. Two replicates were carried out for each measurement.

2. 5. Fourier transform infrared spectroscopy (FTIR) analysis of LEC-based DESs

FTIR spectra of the solid compounds were recorded at 25 °C by a spectrophotometer (Michaelson Bomen MB-series, Canada) using the KBr pastille (1.5 mg/150 mg) technique (4000-400 cm^{-1} range and 2 cm^{-1} resolution). The solid compound and KBr were mixed, vacuumed, and pressed (200 MPa) to form a thin, permeable pastille. The FTIR spectra of the liquid compounds were recorded by the same spectrophotometer with using the special discs.

2. 6. BMSO ethanolysis: equipment and experimental procedure

The reaction of BMSO ethanolysis was performed at 70 ± 0.5 °C under reflux in a magnetically stirred (600 rpm) two-neck round-bottom flask (250 cm^3) placed in a glass chamber. Water temperature in the chamber was kept constant by circulating water from a water bath by a pump. Two series of experiments were performed using calcined and non-calcined CaO. For the first series of experiments, commercial CaO was activated by calcination at 550 °C for 2 h [22], cooled, and kept in well-closed glass bottles in a desiccator with $CaCl_2$ and KOH pellets. The same, not calcined CaO, was used in the second experimental series. For all experiments, ethanol (22.5 g), the catalyst (4 g), and the cosolvent (8 g) were added to the reaction flask. After stirring the suspension for 30 min, BMSO (40 g), previously preheated at the reaction temperature, was poured into the reaction flask, the magnetic stirrer was switched on, and the reaction was timed. The reaction samples (1 cm^3) were taken from the mixture during the reaction at different time intervals, cooled in an ice bath, and centrifuged (Sigma 2-6E, Sigma Laborzentrifugen GmbH, Germany; 3500 rpm, 10 min). The upper ester/oil layer was withdrawn and dissolved in the 2-propanol/*n*-hexane (5:4 v/v) mixture in a 1:10 or 1:200 ratio for qualitative thin layer (TLC) or quantitative liquid chromatography (HPLC) analysis (HPLC chromatograph details: Agilent 1100 Series, Agilent Technologies, Germany), respectively, followed by filtration through a 0.45 µm Millipore filter (Merck KGaA, Germany). After completing the reaction, the reaction mixture was poured into a separation funnel, and the separation of the phases was timed. All experiments were performed twice. For the X-ray powder diffraction (XRD), the precipitated CaO catalyst was removed from the reaction mixture, washed with ethanol, filtered, and dried in an oven at 110 °C for 2 h.

2. 7. Separation of fatty acid ethyl esters (FAEEs)

During the separation of the final reaction mixture, three layers were formed. The upper layer consisted of FAEEs and insignificant amounts of triacylglycerols (TAG), diacylglycerols (DAG), and monoacylglycerols (MAG). The middle layer contained excess ethanol, glycerol, and cosolvent. CaO was precipitated in the bottom layer.

2. 8. Analytical methods

Chemical composition of the reaction mixture samples was analyzed qualitatively and quantitatively by the TLC and HPLC methods, respectively [23,24]. The contents of FAEEs and acylglycerols were calculated from the corresponding peak areas by using the calibration curves obtained by using the standard mixtures. The XRD measurements were performed by using a Philips PW 1050 X-ray powder diffractometer (Philips, The Netherlands) with Ni-filtered Cu $K\alpha_{1,2}$

(λ = 0.154178 nm) radiation and the Bragg-Brentano focusing geometry. Measurements were performed over a 2θ range of 7 to 70° at room temperature. The scanning step was 0.05° the counting time was 3 s per step.

3. RESULTS AND DISCUSSIONS

3. 1. The effect of temperature on the physical properties of LEC-based DESs

3. 1. 1. Density

Figure 1 represents temperature dependences of density of the studied DESs, while the experimental density values are given in Tables A1-A3 in the Supplementary material. The density of the tested LEC-based DESs decreased slightly and linearly with the increase in temperature due to the increased mobility of the molecules and decreased molecular interactions, which agrees with the previous reports [25-27]. For the investigated temperature range, the density of the tested DESs lies within the range of 1285.8 - 1397.6 kg·m^{-3} with the LEC:G DES having the lowest density values. At 313.15 K, all LEC-based DESs are liquid, and their densities follow the following order: LEC:G < LEC:TEOA < LEC:OLA.

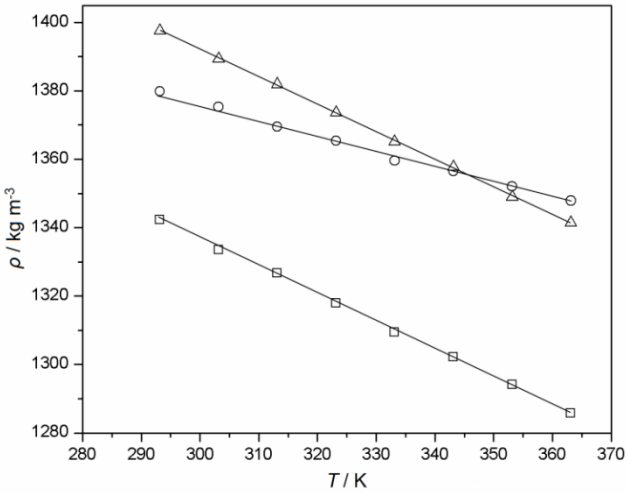

Figure 1. Densities (ρ) of the LEC-based DESs as functions of temperature: LEC:G - □ (STD ≤ 3.5 %), LEC:TEOA - ○(STD ≤ 2.8 %), and LEC:OLA - △(STD ≤ 3.9 %).

Due to the lack of literature data for the tested LEC-based DESs, their density values were compared with those reported for the DESs with the same hydrogen bond donors. Formation of hydrogen bonds between constitutional components of DESs strongly affects the density of all DESs. The LEC:TEOA and LEC:OLA DESs have higher density values than the LEC:G DES due to the highest number of -OH groups in TEOA and the largest molecular size of OLA, providing a stronger intermolecular H-bonds' network as compared to that of the LEC:G DES [28].

The LEC:G DES has a significantly higher density than the DESs with G, such as the *N*,*N*-diethylethanolammonium chloride:G (1:2) [29], tetrapropylammonium bromide:G (1:3) [30], ChCl:G (1:2) DESs [27,31,32] because LEC has the larger molecular mass than the other hydrogen bond acceptors [28]. For the same reason, the density values for the LEC:TEOA DES are higher than those reported for the ChCl:TEOA (1:2) [33] and ChCl:TEOA (1:1) DESs [25].

For the design of technological processes, it is very important to know the effect of temperature on the density of DESs. In addition, density values can be used to calculate values of thermal expansion or compressibility coefficients that are valuable liquid structure and interactions data. When a DES system is heated, the molecules move faster, increasing the molar volume and, thus, decreasing the density [34]. Although high density of a DES is a problem for handling or mixing in chemical processes, it may be desirable in extraction processes since a relatively large difference in density between the raffinate and extract phases is required to guarantee more efficient phase separation [26].

The density values were correlated to the temperature by the following linear equation (1):

$$\rho = a + bT \quad (1)$$

The parameters *a* (the density at 0 K) and *b* (the coefficient of volume expansion) were obtained from the intercept and slope of the best linear fits, respectively (Table 1). The obtained low mean relative percent deviations (MRPD), and coefficients of determination (R^2) close to unity (> 0.996) indicate excellent agreement of the linear density-temperature dependences with experimental data.

Table 1. Parameters obtained by the best linear fits of ρ as a function of temperature in the range 293.15-363.15 K (Eq. 1) for LEC-based DESs

DES	Density range / kg·m^{-3}	*a* / kg·m^{-3}	*b* / kg·m^{-3}·K^{-1}	MRPD, %	R^2
LEC:G	1285.8-1342.3	1577.5	-0.803	0.03	0.999
LEC:TEAO	1347.9-1379.9	1513.6	-0.4581	0.04	0.996
LEC:OLA	1341.4-1397.6	1634	-0.8054	0.02	0.999

According to the values of the coefficient of volume expansion it could be deduced that thermal sensitivities of the LEC-based DESs are in the following order: LEC:OLA > LEC:G > LEC:TEAO.

Expansion of DESs with temperature is best quantified by the thermal expansion coefficient (α), which is obtained as a slope of the ln *ρ*-*T* linear fit of Eq. (2) [25]:

$$\ln \rho = c - \alpha T \quad (2)$$

where *c* is an empirical constant. Thermal expansion coefficient values were determined in the range between $3 \cdot 10^{-4}$ K^{-1} and $6 \cdot 10^{-4}$ K^{-1} (Table 2), indicating that the investigated DESs do not expand appreciably in the covered temperature range.

Table 2. Parameters obtained by the best linear fit of experimental data by Eq. (2) for LEC-based DESs in the temperature range 293.15-363.15 K.

DES	*c* / kg·m^{-3}·K^{-1}	$\alpha \cdot 10^{-4}$/ K^{-1}	MRPD, %	R^2
LEC:G	7.38	6	0.05	0.999
LEC:TEAO	7.33	3	0.16	0.996
LEC:OLA	7.42	6	0.05	0.999

Molar volumes (V_m), lattice energies (U_{pot}), and heat capacities (C_p) for the LEC-based DESs at 313.15 K were calculated using the well-known equations [25,35] and presented in Table 3. The molecular size of OLA induced the highest value of the molar volume of the LEC:OLA DES, which also resulted in its highest heat capacity among all prepared DESs. The liquid state of DESs at lower temperatures can be explained by the lattice energy values similar to those reported for molten salts [36].

Table 3. Calculated values of V_m, U_{pot}, and C_p for the LEC-based DESs at 313.15 K

DES	V_m / nm^3	U_{pot} / kJ·mol^{-1}	C_p / J·mol^{-1}K^{-1}
LEC:G	0.390	1178	450
LEC:TEAO	0.424	1141	485
LEC:OLA	0.528	1048	593

3. 1. 2. Refractive index

The refractive index is correlated with temperature as shown in Figure 2, while the experimental refractive index values are given in Tables A1-A3 in the Supplementary material. The refractive indices of the tested LEC-based DESs linearly decreased with temperature due to the reduction in density. This decrease strongly depends on the structure and nature of the constitutional components combined with LEC. The refractive index values for the investigated temperature range lie within 1.4305-1.4853, with the LEC:OLA DES having the lowest refractive index. At 313.15 K, these values are in the following order: LEC:OLA < LEC:G < LEC:TEOA and are higher than those reported for *N*,*N*-di-ethylethanolammonium chloride:G [29], and ChCl:G (1:2) [32] DESs. At the same time, they are close to those reported for tetrapropylammonium bromide:G (1:2) [30] and ChCl:G (1:2) [27] DESs.

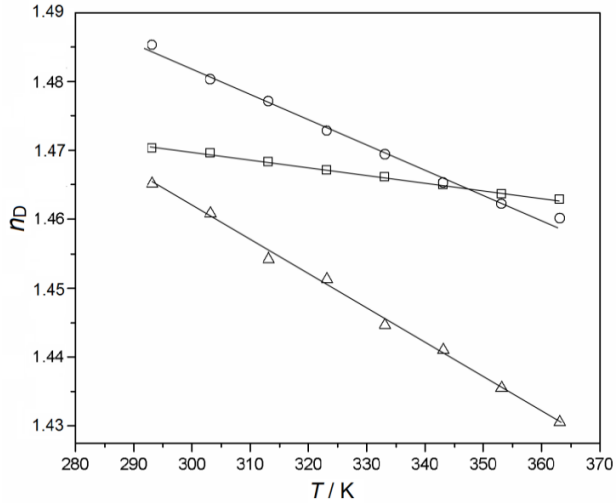

Figure 2. Refractive indices (n_D) of the LEC-based DESs as functions of temperature: LEC:G - ☐ (STD ≤ 0.05 %), LEC:TEOA - ○ (STD ≤ 0.07 %), and LEC:OLA - △ (STD ≤ 0.11 %).

Refractive index is a property beneficial for many applications, such as identification of individual substances and determination of their concentrations in mixtures, verification of the substance purity, *etc.* [37]. The determined parameters of linear dependences, refractive index ranges, MRPD, and R^2 are listed in Table 4.

Table 4. Parameters obtained by the best linear fits of n_D as a function of temperature in the range 293.15-363.15 K for the LEC-based DESs

DES	n_D range	Intercept	Slope	MRPD, %	R^2
LEC:G	1.4628-1.4703	1.5031	-0.0001	1.98	0.997
LEC:TEAO	1.4601-1.4853	1.591	-0.0004	0.80	0.993
LEC:OLA	1.4305-1.4651	1.61	-0.0005	0.13	0.997

Values of the phase velocity (υ), molar refractivity (A), and the free volume (f_m), calculated using the well-known equations, are listed in Table 5 [38,39]. The lowest LEC:OLA DES refraction index values are explained by the lowest phase velocity values. The molar refractivity is mainly affected by the molar mass, while it is only weakly affected by temperature [39]. Also, the influence of density and refraction index is only minor [39]. Heating causes an increase in the free volume of DESs [39]. The highest free volume values determined for the LEC:OLA DES can be explained by the longest alkyl chain of OLA [39].

Table 5. The υ, A, and f_m ranges determined for the LEC-based DESs in the temperature range 293.15-363.15 K.

DES	υ / 10^7 m·s^{-1}	A / 10^{-6} m^3·mol^{-1}	f_m / 10^{-6} m^3·mol^{-1}
LEC:G	20.40-20.51	64.86-66.78	167.48-175.77
LEC:TEAO	20.20-20.55	84.76-86.94	180.97-188.60
LEC:OLA	20.48-20.97	71.16-72.76	227.48-242.88

3. 1. 3. Viscosity

Knowing viscosity of solvents is of great importance for their further applications in technological processes. High viscosity of DESs poses a significant problem due to reduction of the mass transfer rate, which can be overcome by heating or modifying molar ratios of the DES components [26]. The viscosity values obtained in the present work were correlated with temperature by both the Arrhenius (Eq. 3) [25] and Vogel-Tamman-Fulcher (VTF) (Eq. 4) [40] equations (Fig. 3). The experimental viscosity values are presented in Tables D1-D3 of the Supplementary material. Evidently, the viscosity decreases with the temperature increase, probably due to breaking the hydrogen bonds in DESs. For the investigated temperature range, the viscosity values of the tested DESs lie within the range of 0.588-22.369 Pa·s. At temperatures up to 283.15 K, the LEC:G DES is solid. The viscosity values of the LEC-based DESs at 313.15 K are in the following order: LEC:OLE < LEC:TEOA < LEC:G.

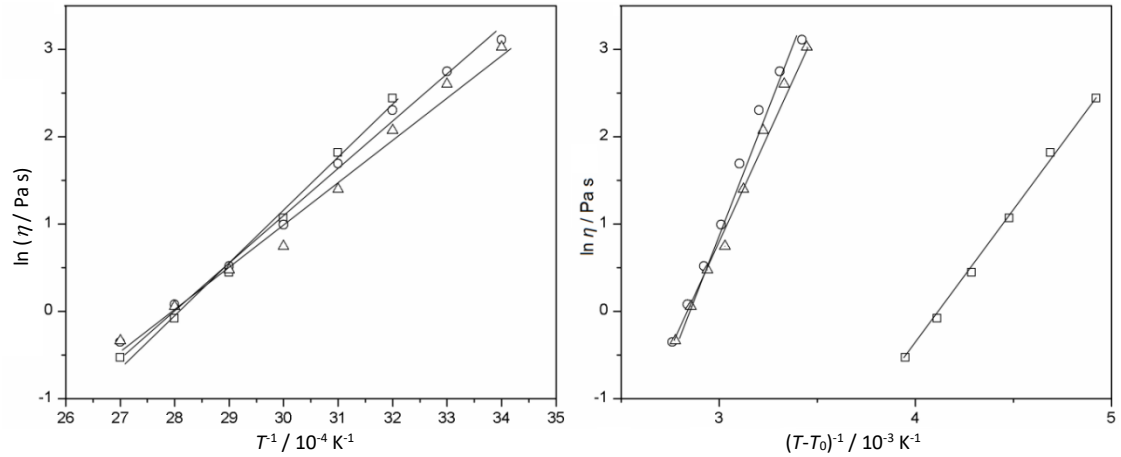

Figure 3. Logarithmic dependences of viscosity (η) of the LEC-based DESs on temperature and application of: a) Arrhenius equation; b) VTF equation (LEC:G - □ (STD ≤ 0.03), LEC:TEOA - ○ (STD ≤ 0.02) and LEC:OLA - △(STD ≤ 0.03))

As expected, the LEC-based DESs are highly viscous at lower temperatures. Due to heating, the constituents move faster, thus reducing the viscosity value [26]. To eliminate the negative viscosity effect on the technological process, these DESs should be used at temperatures higher than 313.15 K. The LEC:G DES exhibits higher viscosity than the *N*,*N*-diethylethanolammonium chloride:G (1:2) [29], tetrapropylammonium bromide:G (1:3) [30] and ChCl:G (1:2) [27,31,32] DESs.

In the Arrhenius equation (3):

$$\ln \eta = \ln A_\eta + (E_\eta/RT) \quad (3)$$

η, T, E_η, A_η, and R represent the viscosity, the absolute temperature, the activation energy for the viscous flow, the pre-exponential constant, and the universal gas constant, respectively; values of these parameters are shown in Table 6.

Table 6. Parameters of the Arrhenius-type equation for the LEC-based DESs in the temperature range 293.15-363.15 K.

DES	Viscosity range, Pa·s	Arrhenius equation (η / Pa·s; T / K)	A_η / μPa s	E_η / J·mol^{-1}	MRPD, %	R^2
LEC:G	0.588-11.457	$\ln \eta = 6891.8T^{-1}$-19.5	0.180	57298	10.32	0.997
LEC:TEAO	0.702-22.369	$\ln \eta = 5523.1T^{-1}$-15.5	0.004	45919	11.22	0.990
LEC:OLA	0.711-20.610	$\ln \eta = 5308.0T^{-1}$-15.0	0.305	44131	12.71	0.993

The VTF equation (4) is expressed as:

$$\eta = \eta_0 \exp \frac{B_\eta}{T - T_0} \quad (4)$$

The values of T_0 (so-called ideal glass-transition temperature), η_0 (adjustable parameter), and B_η (factor related to the activation energy) are listed in Table 7.

Table 7. Parameters of the VTF equation for the LEC-based DESs in the temperature range 293.15-363.15 K.

DES	VTF equation (η / Pa·s; T / K)	η_0 / Pa s	B_η / K	T_0 / K	MRPD, %	R^2
LEC:G	$\ln \eta$=3118.4$(T-T_0)^{-1}$-12.88	2.528·10^{-6}	3118	110	8.01	0.998
LEC:TEAO	$\ln \eta$=5489$(T-T_0)^{-1}$-15.47	1.899·10^{-7}	5489	1	11.35	0.990
LEC:OLA	$\ln \eta$=5210.4$(T-T_0)^{-1}$-14.85	3.543·10^{-7}	5210	3	12.67	0.993

To get more information about DESs viscous flow, the equation (5) is used [25]:

$$\ln \frac{\eta V}{hN_A} = \frac{\Delta H^*}{RT} - \frac{\Delta S^*}{R} \quad (5)$$

where V - the molar volume of DES (the ratio of average M_{DES} and density of the DES at desired temperature), N_A - the Avogadro's number; h - the Planck's constant; ΔH^* -viscous flow activation enthalpy; R - universal gas constant; ΔS^* - activation entropy of viscous flow. The plots of ln ($\eta V/hN_A$) *vs*. the inverse temperature are shown in Figure 4, while the values of R^2, ΔH^*, $T\Delta S^*$, and ΔG^* for the LEC-based DESs at 313.15 K are listed in Table 8. The DESs values of the viscous

flow activation enthalpy were greater than the $T\Delta S^*$ values. These facts indicate that the energetic contribution due to the viscous flow activation enthalpy is more significant than the entropic input to the activation Gibbs energy.

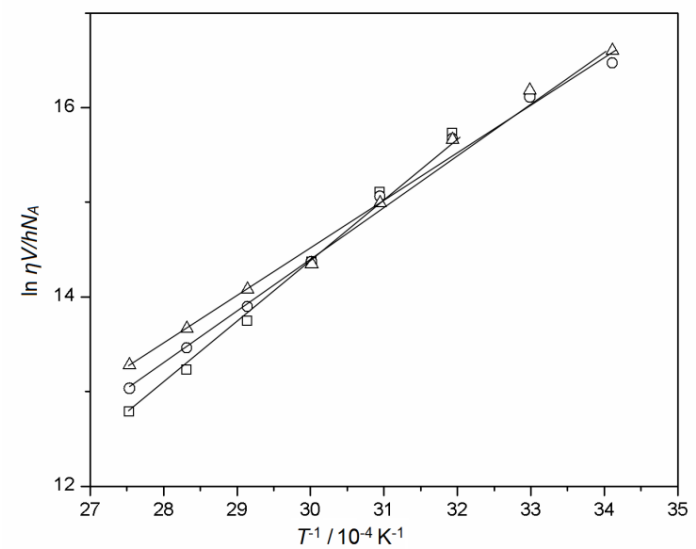

Figure 4. The plot of ln ($\eta V/hN_A$) vs. inverse temperature for LEC-based DESs: experimental data (LEC:G - □ (STD ≤ 0.3), LEC:TEOA - ○ (STD ≤ 0.5) and LEC:OLA - △ (STD ≤ 0.9)) and the best linear fits (lines)

Table 8. Values of R^2, ΔH^*, $T\Delta S^*$, and ΔG^* determined for the LEC-based DESs at 313.15 K

DES	Eyring's equation (T / K)	R^2	ΔH^* / kJ·mol^{-1}	$T\Delta S^*$ / kJ·mol^{-1}	ΔG^* / kJ·mol^{-1}
LEC:G	$\ln(\eta V_m/hN_A) = 6821.4T^{-1} - 4.9$	0.997	56.7	-12.9	43.8
LEC:TEAO	$\ln(\eta V_m/hN_A) = 5487.2T^{-1} - 0.9$	0.990	45.6	-2.4	43.2
LEC:OLA	$\ln(\eta V_m/hN_A) = 5245.4T^{-1} - 0.2$	0.993	43.6	-0.5	43.1

3. 1. 4. FTIR spectra

The FTIR spectra of LEC and the investigated DESs are shown in Figure 5.

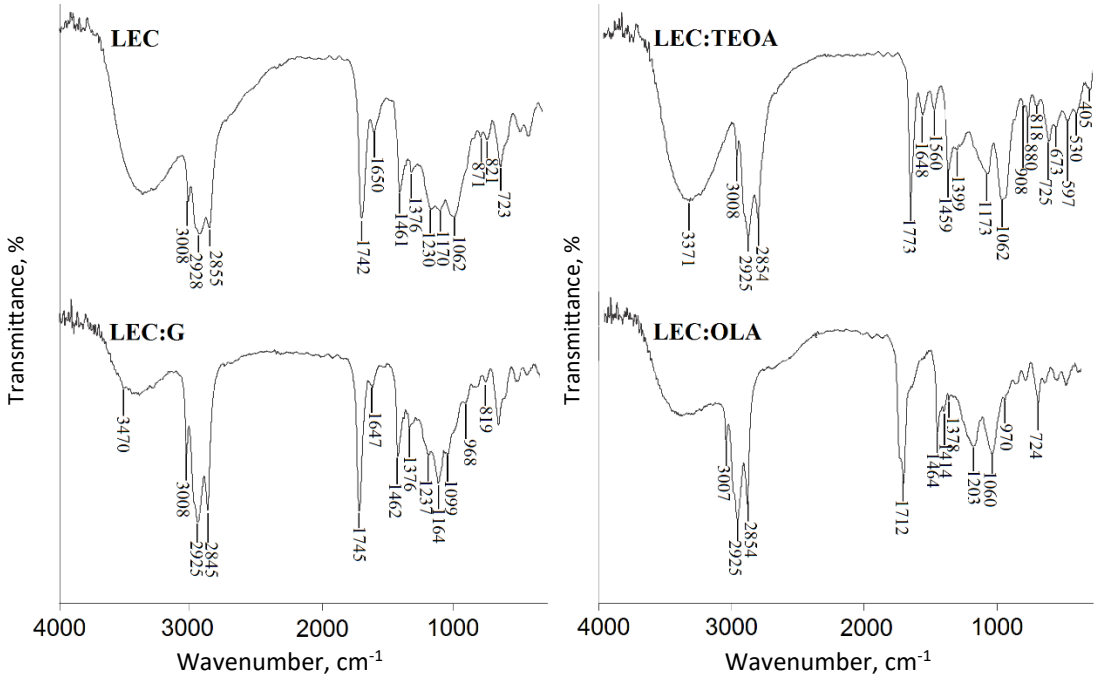

Figure 5. FTIR spectra of the LEC and the investigated LEC-based DESs (25 °C, 400-4000 cm^{-1})

The spectra of the DESs show an intensive broadband at 3200-3500 cm^{-1} due to stretching *ν*(OH) vibrations. The shape and position suggest the existence of hydrogen bonds. This band is intensive in the spectra of all starting components of DESs except for the OLE spectrum since the long carbon chain does not allow the formation of intramolecular hydrogen bonds. The amine vibrations present in the spectrum of TEOA are covered by the stretching vibrations of hydroxyl groups [41]. The FTIR spectra of the DESs and their constituents [41] show stretching *ν*(C-H) vibrations at 2800-3000 cm^{-1}. The intensive band at 1712 to 1773 cm^{-1} in the spectra of all DESs originates from the stretching *ν*(C=O) vibrations characteristic for the spectrum of LEC. The bending *δ*(OH) vibrations at 1660-1647 cm^{-1} in the spectra of the LEC:G and LEC:TEOA DESs overlap the bending *δ*(NH_3^+) vibration at 1660 cm^{-1} in the spectrum of TEOA. Bending *δ*(C-H) vibrations at 1376 to 1474 cm^{-1} are present in all spectra. Bands originating from the stretching *ν*(C-O) vibrations are present in all spectra at 1170 to 1287 cm^{-1}. The bands arising from the POC and PO_2 groups in LEC overlap in the spectrum of LEC and are visible in all spectra of the DESs at 1060 to 1099 cm^{-1}. The FTIR analysis shows the presence of characteristic functional groups of LEC-based DESs constituents, proving that the preparation of DESs does not lead to their chemical changes. Also, the FTIR analysis shows the presence of hydrogen bonds created in the investigated DESs.

3. 2. CaO-catalyzed ethanolysis of BMSO

Figure 6 presents FAEE contents during the CaO-catalyzed BMSO ethanolysis in the presence of DESs or each component, compared to the control reaction in the absence of any cosolvent. BMSO and ethanol did not react in the absence of CaO catalyst, indicating that the tested DESs did not exhibit catalytic activity. The CaO-catalyzed ethanolysis of BMSO without any cosolvents provides a three-phase system, so the sigmoidal dependence of the FAEE content with time is typical due to the mass transfer limitations and the slow TAG conversion at the start of the reaction [4,42,43].

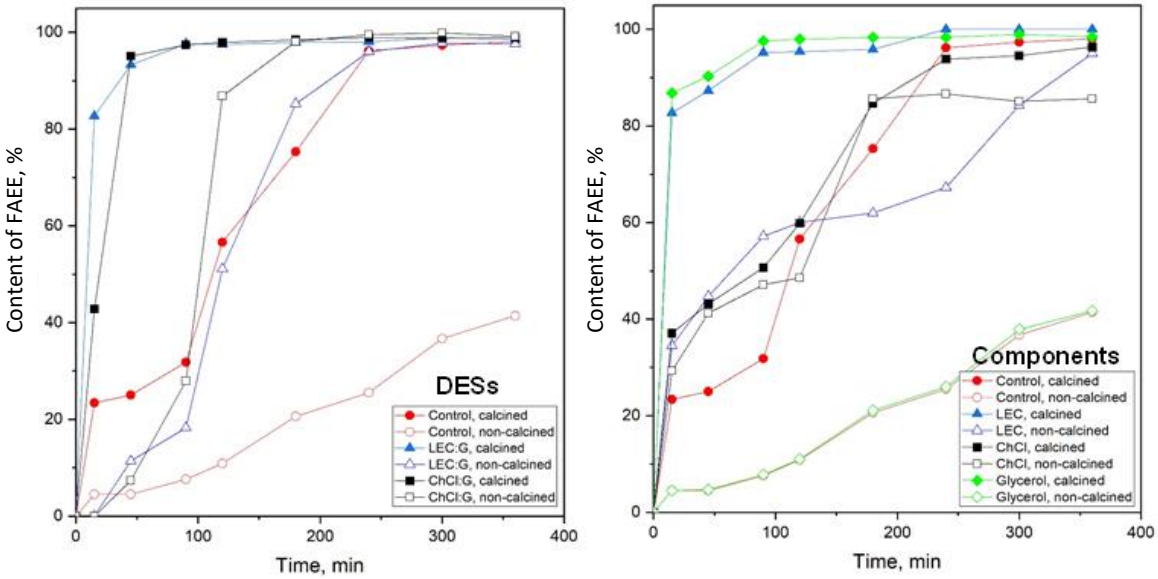

Figure 6. Effects of the LEC- and ChCl-based DESs or their constituents on the FAEE content during the ethanolysis of BMSO catalyzed by non-calcined (open symbols) or calcined (filled symbols) CaO (reaction conditions: temperature 70 °C, ethanol-to-oil molar ratio 12:1, the amounts of DES and CaO to BMSO: 20 and 10 wt.%; average STD ≤ 1.56 (left) and 1.41 (right))

Calcined CaO has shown a more intensive catalytic activity as compared to the non-calcined CaO due to the removal of CO_2 and H_2O from the catalyst particles in the former case by calcination as these components are considered poisonous to the catalyst active sites. As a result, the FAEE content in the presence of calcined CaO rose to 96.2±1.2 % within 4 h; further prolongation of the reaction resulted in a negligible increase in the FAEE content. On the contrary, in the presence of non-calcined CaO, high FAEE content was not achieved even after 6 h of the reaction.

The LEC:G and ChCl:G DESs accelerated the BMSO ethanolysis over both catalysts. A more positive influence of the hydrophobic LEC:G DES on the calcined CaO-catalyzed reaction was observed after only 15 min reaching the FAEE

content of 82.7±1.8 %, as compared to that reported for the hydrophilic ChCl:G DES (42.8±4.5 %) [4]. However, the efficiency of these DESs was similar after 45 min, with FAEE contents of 93.3±0.9 and 95.1±2.5 % for the system containing the LEC:G and ChCl:G DES, respectively. Maximal FAEE contents of 97.6±0.6 and 97.4±1.2 % for the LEC:G and ChCl:G DES, respectively, were achieved after 90 min. Further prolongation of the reaction resulted in a negligible increase in the FAEE content (97.9±1.5 and 98.1±0.7 %, respectively, after 3 h).

In the reaction catalyzed by non-calcined CaO, the presence of the LEC:G and ChCl:G DESs as cosolvents provided FAEE contents of 96.0±1.1 and 98.1 % after 3 h, respectively. On the other hand, LEC, ChCl, and G were less efficient cosolvents used with the same catalyst, resulting in FAEE contents of 84.32±1.7, 81.09±0.8, and 26.0±3.1 %, respectively, for the same duration of the transesterification.

Positive effects of the ChCl:G DES as a cosolvent in CaO-catalyzed transesterification of vegetable oils have already been reported [4,44]. The results obtained in the present study indicate that the LEC:G DES can successfully activate CaO, providing a more cost-effective procedure than thermal activation.

3. 3. Separation of FAEEs

Addition of the LEC- or ChCl-based DESs in the BMSO ethanolysis accelerated the phase separation of the final reaction mixture (30 min) as compared to the control reaction in the absence of any cosolvent (more than 12 h). Also, the presence of these DESs in reaction systems may cause the reduction of soap formation, as noticed for the ethanolysis of other oily feedstocks [4,45,46]. However, the systems containing CaO without and with LEC, ChCl, or G remained very viscous and separated much slower.

3. 4. XRD of the used CaO catalyst

Figures 7-9 show XRD spectra of the initial and used non-calcined and calcined CaO samples separated from the final reaction mixtures of the BMSO ethanolysis conducted in the presence of the LEC:G and ChCl:G DESs or their constituents (LEC, ChCl, and G).

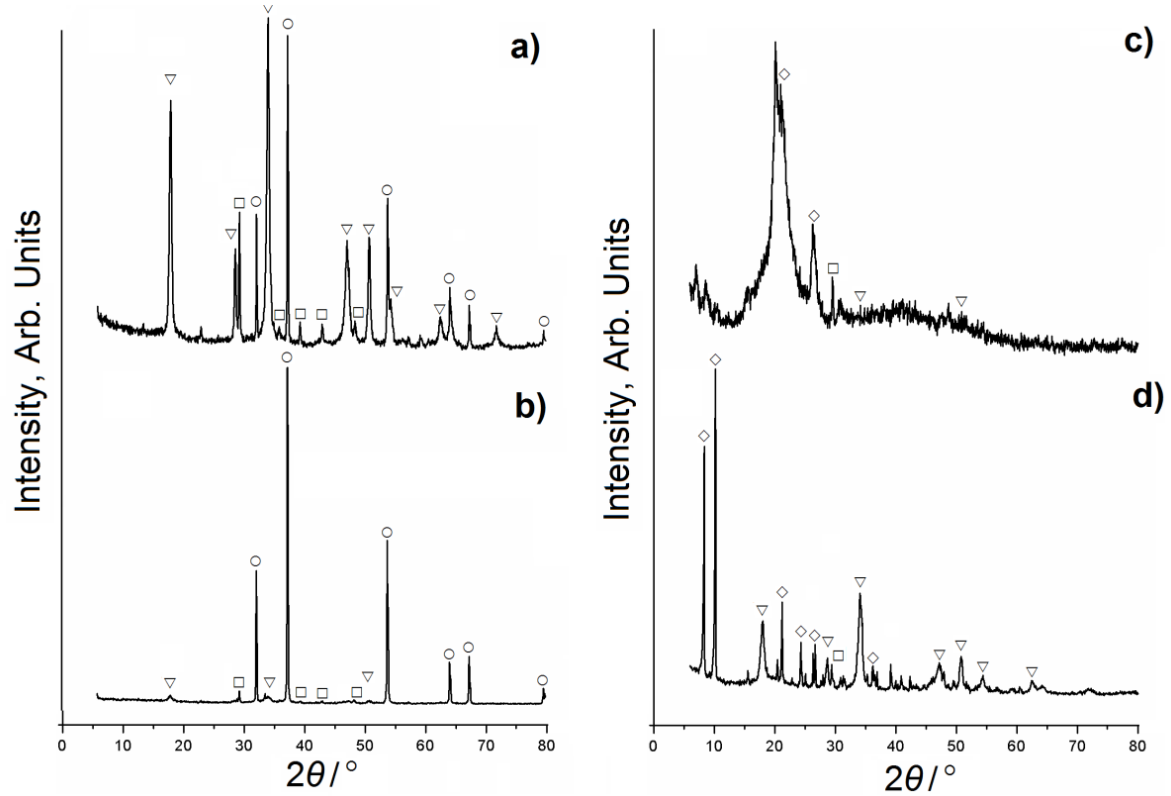

Figure 7. XRD patters of the fresh non-calcined (a) and calcined (b) CaO samples and the used non-calcined (c) and calcined (d) CaO pastes recovered from the reaction mixture after 6 h (○ - CaO, ▽ - $Ca(OH)_2$, □ - $CaCO_3$, ◇ - CaDG (calcium diglyceroxide)).

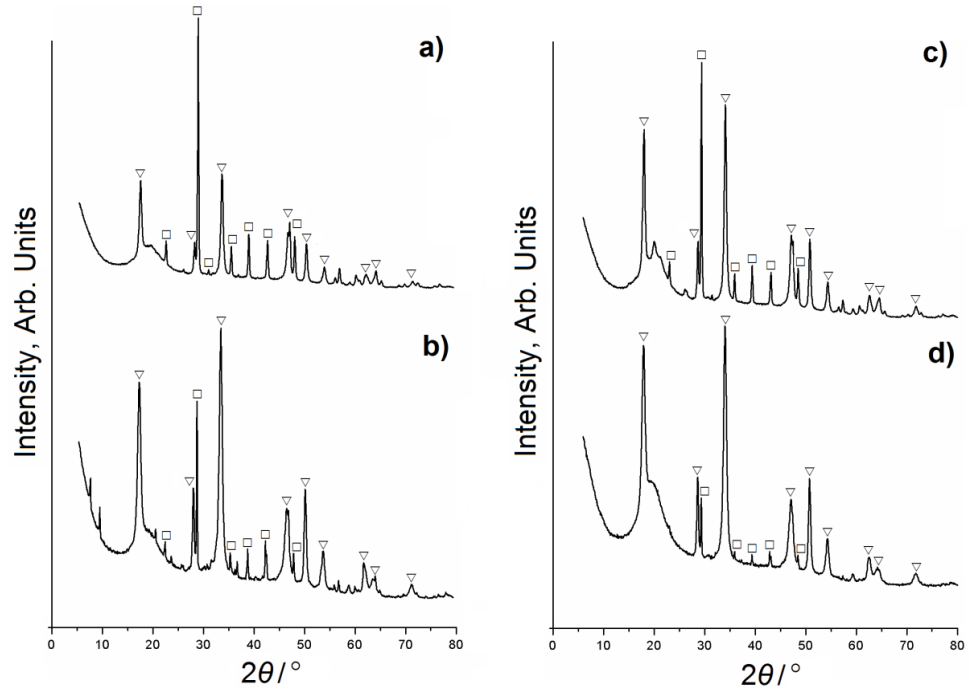

Figure 8. XRD patters of the used non-calcined (a,c) and calcined (b,d) CaO samples taken after 6 h from the ethanolysis reaction carried out in the presence of LEC:G (a,b) and ChCl:G (c,d) DESs (○ - CaO, ▽ - $Ca(OH)_2$, □ - $CaCO_3$)

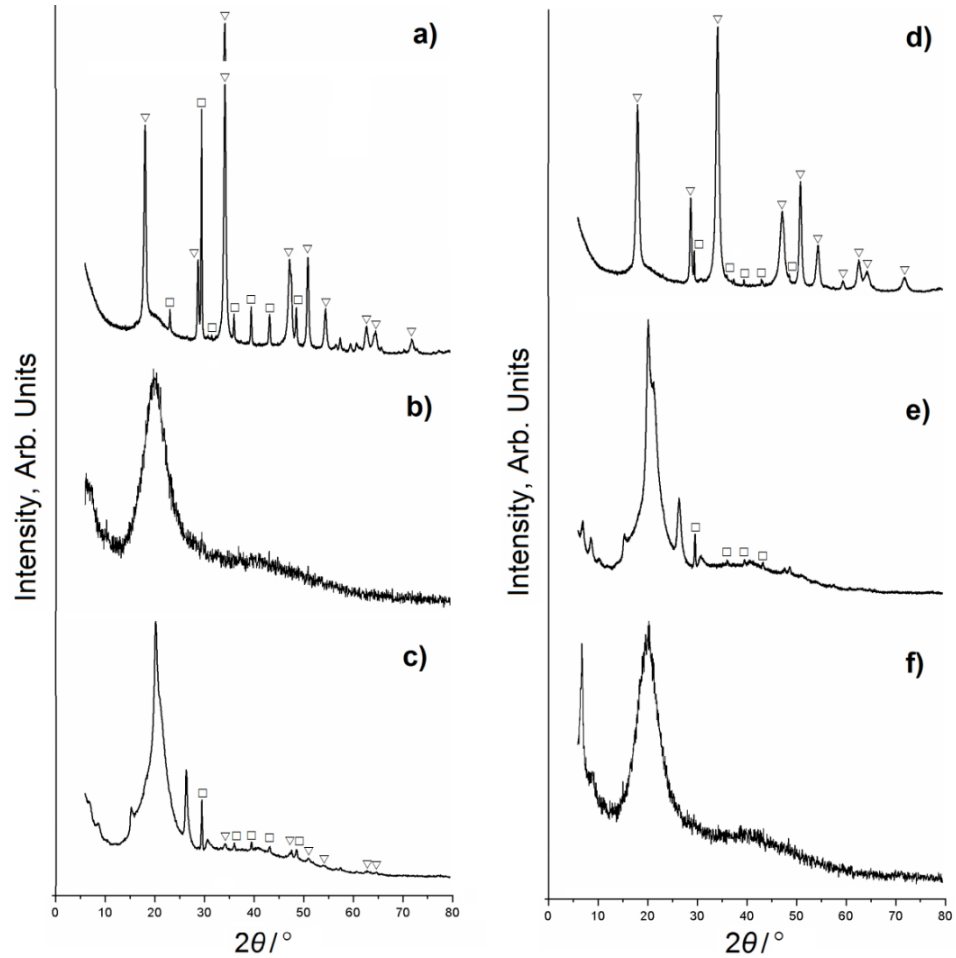

Figure 9. XRD patterns of the used non-calcined (a,c,e) and calcined (b,d,f) CaO samples taken after 6 h from the ethanolysis reaction carried out in the presence of LEC (a,b), ChCl (c,d) or G (e,f) (○ - CaO, ▽ - $Ca(OH)_2$, □ - $CaCO_3$)

The XRD analysis of the non-calcined CaO sample revealed the peaks attributed to the CaO phase (2θ = 32.22 (32.4), 37.36 (37.55), 53.86 (54.05), 64.16 (64.35), and 67.38 (67.55)°, JCPDS Card 43-1001), $Ca(OH)_2$ phase (2θ = 18.15 (17.98), 34.25 (34.1), 47.3 (47.18), 51, 62.75 and 64.35°, JCPDS Card 84-1263), and $CaCO_3$ phase (2θ = 29.5 and 43.14°, JCPDS Card 81-2027). The presence of the $CaCO_3$ and $Ca(OH)_2$ peaks was attributed to the sensitivity of CaO towards atmospheric moisture and CO_2.

The fresh calcined CaO sample appeared as an almost single well-crystallized CaO phase with minor peaks characteristic for the $Ca(OH)_2$ phase (2θ = 18.15 (17.98), 34.25 (34.1), 47.3 (47.18), 51, 62.75 and 64.35°), and $CaCO_3$ phase (2θ = 29.5 and 43.14°), confirming the CaO activation by calcination.

There were apparent changes in the XRD patterns of calcined and non-calcined CaO used in the BMSO ethanolysis without or with cosolvents. However, a major difference was due to the absence of the CaO phase, which was converted into $Ca(OH)_2$ and $CaCO_3$ during the hydration and carbonation processes during the collection step [4, 47].

The calcined CaO sample collected from the reactions carried out in the absence of any cosolvent revealed the presence of calcium diglyceroxide (2θ = 8.5 (8.2), 10.4 (10.2), 21.3 (21.2), 24.4, 26.6, 34.4, and 36.2°, PDF#21-1544) along with $Ca(OH)_2$ (2θ = 17.94 (17.98), 28.7 (28.72), 34.08 (34.12), 47.16 (47.18), 50.8 (50.84), 54.54, 59.4, and 62.62 (62.64)°), and $CaCO_3$ (2θ = 29.4 (28.8)°). The XRD spectrum indicated transformation of the majority of the CaO catalyst into calcium diglyceroxide with the by-produced G in the successful CaO-catalyzed transesterification, CaO particles are transformed into $Ca(OH)_2$ in the initial stage. In contrast, in the last stage, these particles become calcium-diglyceroxide [48,49].

Although these phases are also seen in the XRD spectra of the used non-calcined CaO catalyst, the presence of the amorphous phase (a broad peak with a maximum at about 2θ = 20°) was also observed. This peak could originate from calcium ethoxide (produced in the catalyst preparation step when the calcined CaO/ethanol mixture was stirred at 70 °C for 30 min) or be attributed to the deposition of organic molecules on the surface of the used CaO catalyst [47].

In the XRD spectra of non-calcined and calcined CaO used in the reaction with the addition of different DESs or their constituents, the presence of $Ca(OH)_2$ and $CaCO_3$ phases was evident, while calcium diglyceroxide was not identified. Furthermore, the peak at about 2θ = 20.5° was more pronounced in the catalytic systems with the constituents of the DESs, suggesting that the synthesized amount of calcium diglyceroxide was quite low and insufficient for detection by the XRD apparatus.

It should be noted that the absence of peaks characteristic for calcium diglyceroxide could be explained by its low amount (*i.e.*, insufficient to surpass the XRD apparatus limit detection), easy dissolution [50], and instability, causing calcium leaching into the reaction medium [49]. Solubilization of calcium diglyceroxide in alcohol might also produce a soluble precursor, which could be later transformed into the final solid base catalyst [51]. Moreover, amorphization of calcium ethoxide during the catalyst drying [52] would result in the presence of only $Ca(OH)_2$ and $CaCO_3$ phases in the XRD spectra. Amorphisation was also reported after the reactions in which other calcium-based catalysts prepared by calcination of animal waste were used [53].

4. CONCLUSION

Three novel DESs were prepared by combining LEC with G, TEOA, or OLE in 1:2 molar ratio. Densities, viscosities, and refractive indices of the tested DESs decreased with the increase in temperature applied in the range 293.15-363.15 K at the atmospheric pressure relevant for practical applications. All tested LEC-based DESs are liquid at 313.15 K. The FTIR spectra of LEC and investigated LEC-based DESs indicated absence of chemical reactions during the DES preparation. The LEC:G and ChCl:G DESs were further used for ethanolysis of cold-pressed BMSO catalyzed by non-calcined or calcined CaO. Both DESs were shown to successfully activate the non-calcined CaO catalyst providing the FAEE contents of over 96.5 % after 3 h. However, in the presence of these DESs in the reaction catalyzed by calcined CaO, the FAEE contents above 96.5 % were obtained after 90 min. The hydrophobic LEC:G DES proved to be a more successful cosolvent than the hydrophilic ChCl:G prepared in the same molar ratio (1:2) at the beginning of the reaction, while after 45 min of the reaction, their efficiencies were similar. Both DESs accelerated separation of the esters from the final reaction mixture. This study proved that DESs composed of natural, safe, cheap, available, biodegradable and environmental-friendly compounds may serve as efficient cosolvents and/or activators of heterogeneous alkaline

catalyst for transesterification reaction. Thus, further investigation should be focused on improving the reaction by using other non-edible or waste oils and fats, additionally reducing the cost of the process and enabling successful industrialization of biodiesel production.

Acknowledgement: This work has been funded by the Republic of Serbia - Ministry of Education, Science and Technological Development, Program for financing scientific research work, number 451-03-68/2022-14/200133. This research is also a part of the Project 0-14-18 (Development, modeling, and optimization of biodiesel production from non-edible and waste feedstocks) of the SASA Branch in Niš, Serbia.

REFERENCES

[1] Bergua F, Delso I, Muñoz-Embid J, Lafuente C, Artal M. Structure and properties of two glucose-based deep eutectic systems. *Food Chem.* 2021; 336: 127717. https://doi.org/10.1016/j.foodchem.2020.127717

[2] Balaraman HB, Rathnasamy SK. Kinetics and microwave-assisted extractive transesterification studies of high octane methyl esters (HOME) from karanja and chicken lard oil using protic deep eutectic solvent. *Fuel*. 2020; 268: 117299. https://doi.org/10.1016/j.fuel.2020.117299

[3] Manurung R, Taslim T, Siregar AGA. Deep eutectic solvents based choline chloride for enzymatic biodiesel production from degumming palm oil. *Asian J. Chem.* 2020; 3: 733-738. https://doi.org/10.14233/ajchem.2020.22193

[4] Troter DZ, Todorović ZB, Đokić-Stojanović DR, Veselinović LjM, Zdujić MV, Veljković VB. Choline chloride-based deep eutectic solvents in CaO-catalyzed ethanolysis of expired sunflower oil. *J Mol Liq.* 2018; 266: 557-567. https://doi.org/10.1016/j.molliq.2018.06.106

[5] Merza F, Fawzy A, AlNashef I, Al-Zuhair S., Taher H. Effectiveness of using deep eutectic solvents as an alternative to conventional solvents in enzymatic biodiesel production from waste oils. *Energy Rep.* 2018; 4: 77-83. https://doi.org/10.1016/j.egyr.2018.01.005

[6] Gu L, Huang W, Tang S, Tian S, Zhang X. A novel deep eutectic solvent for biodiesel preparation using a homogeneous base catalyst. *Chem Eng Sci.* 2015; 259: 647-652. https://doi.org/10.1016/j.cej.2014.08.026

[7] Zhang Y, Xia X, Duan M, Han Y, Liu J, Luo M, Zhao C, Zu Y, Fu Y. Green deep eutectic solvent assisted enzymatic preparation of biodiesel from yellow horn seed oil with microwave irradiation. *J Mol Catal B Enzym.* 2016; 123: 35-40. https://doi.org/10.1016/j.molcatb.2015.10.013

[8] Alam MM, Rahman KA. Biodiesel from mustard oil: a sustainable engine fuel substitute for Bangladesh. *Int J Renew Energy Dev.* 2013; 2: 141-149. https://doi.org/10.14710/ijred.2.3

[9] Đorđević BS, Troter DZ, Todorović ZB, Đalović IG, Stanojević LjP, Mitrović PM, Veljković VB. The effect of the triethanolamine: glycerol deep eutectic solvent on the yield, fatty acid composition, antioxidant activity, and physicochemical properties of black mustard (*Brassica nigra* L.) seed oil. *J Food Meas Charact.* 2020; 14: 2570-2577. https://doi.org/10.1007/s11694-020-00503-3

[10] Aslan V, Eryilmaz T. Polynomial regression method for optimization of biodiesel production from black mustard (*Brassica nigra* L.) seed oil using methanol, ethanol, NaOH, and KOH, *Energy.* 2020; 209: 118386. https://doi.org/10.1016/j.energy.2020.118386

[11] Knothe G. Dependence of biodiesel fuel properties on the structure of fatty acid alkyl esters. *Fuel Process Technol.* 2005; 86: 1059–70. https://doi.org/10.1016/j.fuproc.2004.11.002

[12] Shahzadi I, Sadaf S, Iqbal J, Ullah I, Bhatti HN. Evaluation of mustard oil for the synthesis of biodiesel: Pretreatment and optimization study. *Environ Prog Sustain Energy.* 2018; 37: 1829-1835. https://doi.org/10.1002/ep.12833

[13] Robert C, Couëdelo L, Vaysse C, Michalski M-C. Vegetable lecithins: a review of their compositional diversity, impact on lipid metabolism and potential in cardiometabolic disease prevention. *Biochimie*. 2020; 169: 121-132. https://doi.org/10.1016/j.biochi.2019.11.017

[14] Jung Y-G, Lee C-R, Kim H-J, Kim Min-G, Jin KS, Lee H-Y. Effect of hydrocarbon chain length of aliphatic solvents on the reverse self-assembly of lecithin and monovalent ion mixtures. *Colloids Surf A Physicochem Eng Asp.* 2020; 607: 125441. https://doi.org/10.1016/j.colsurfa.2020.125441

[15] Tung SH, Huang YE, Raghavan SR. A new reverse wormlike micellar system: mixtures of bile salt and lecithin in organic liquids. *J Am Chem Soc.* 2006; 128: 5751-5756. https://doi.org/10.1021/ja0583766

[16] Kumar R, Katare OP. Lecithin organogels as a potential phospholipid-structured system for topical drug delivery: a review. *AAPS PharmSciTech*. 2005; 6: 298-310. https://doi.org/10.1208/pt060240

[17] Zou H, Zhao N, Li S, Sun S, Dong X, Yu C. Physicochemical and emulsifying properties of mussel water-soluble proteins as affected by lecithin concentration. *Int J Biol. Macromol.* 2020; 163: 180-189. https://doi.org/10.1016/j.ijbiomac.2020.06.225

[18] Amiri-Rigi A., Abbasi S. Extraction of lycopene using a lecithin-based olive oil microemulsion. *Food Chem.* 2018; 272: 568-573. https://doi.org/10.1016/j.foodchem.2018.08.080

[19] Shen Y, Chang C, Shi M, Su Y, Gu L, Li J, Yang Y. Interactions between lecithin and yolk granule and their influence on the emulsifying properties. *Food Hydrocoll.* 2019; 101: 105510. https://doi.org/10.1016/j.foodhyd.2019.105510

[20] Xue J, Zhong Q. Thyme oil nanoemulsions coemulsified by sodium caseinate and lecithin. *J Agric Food Chem.* 2014; 62: 9900-9907. https://doi.org/10.1021/jf5034366

[21] Đorđević BS., Todorović ZB, Troter DZ, Stanojević LjP, Veljković VB. Extraction of quercetin from waste onion (*Allium cepa* L.) tunic by the aqueous solutions of different deep eutectic solvents. *Adv Technol.* 2018; 7: 5-10. https://doi.org/10.5937/SavTeh1802005d

[22] Veljković VB, Stamenković OS, Todorović ZB, Lazić ML, Skala DU. Kinetics of sunflower oil methanolysis catalyzed by calcium oxide. *Fuel.* 2009; 88: 1554-1562. https://doi.org/10.1016/j.fuel.2009.02.013

[23] Stamenkoviæ OS, Rajkoviæ K, Velièkoviæ AV, Miliæ PS, Veljkoviæ VB. Optimization of base-catalyzed ethanolysis of sunflower oil by regression and artificial neural network models. *Fuel Process Technol.* 2013; 114: 101-108. https://doi.org/10.1016/j.fuproc.2013.03.038

[24] Veličković AV, Stamenković OS, Todorović ZB, Veljković VB. Application of the full factorial design to optimization of base-catalyzed sunflower oil ethanolysis. *Fuel.* 2013; 104: 433-442. https://doi.org/10.1016/j.fuel.2012.08.015

[25] Constantin V, Adya AK, Popescu A-M. Density, transport properties and electrochemical potential windows for the 2-hydroxy-*N,N,N*-trimethylethanaminium chlorides based ionic liquids at several temperatures. *Fluid Phase Equilib.* 2015; 395: 58-66. https://doi.org/10.1016/j.fluid.2015.03.025

[26] Mitar A, Panić M, Prlić Kardum J, Halambek J, Sander A, Zagajski Kučan K, Radojčić Redovniković I, Radošević K. Physicochemical properties, cytotoxicity, and antioxidative activity of natural deep eutectic solvents containing organic acid. *Chem Biochem Eng Q.* 2019; 33: 1-18. https://doi.org/10.15255/CABEQ.2018.1454

[27] Troter DZ, Todorović ZB, Đokić-Stojanović DR, Đordević BS, Todorović VM, Konstantinović SS, Veljković VB. The physicochemical and thermodynamic properties of the choline chloride-based deep eutectic solvents. *J Serbian Chem Soc.* 2017; 82: 1039-1052. https://doi.org/10.2298/jsc170225065t

[28] *Ramón DJ, Guillena G. Deep Eutectic Solvents: Synthesis, Properties, and Applications,* John Wiley & Sons; *2020;* 1-21.

[29] Siongco KR, Leron RB, Li M-H. Densities, refractive indices, and viscosities of *N,N*-diethylethanol ammonium chloride-glycerol or -ethylene glycol deep eutectic solvents and their aqueous solutions. *J Chem Thermodyn.* 2013; 65: 65-72. https://doi.org/10.1016/j.jct.2013.05.041

[30] Jibril B, Mjalli F, Naser J, Gano Z. New tetrapropylammonium bromide-based deep eutectic solvents: Synthesis and characterizations. *J Mol Liq.* 2014; 199: 462-469. https://doi.org/10.1016/j.molliq.2014.08.004

[31] AlOmar MK, Hayyan M, Alsaadi MA, Akib S, Hayyan A, Hashim MA. Glycerol-based deep eutectic solvents: Physical properties. *J Mol Liq.* 2016; 215: 98-103. https://doi.org/10.1016/j.molliq.2015.11.032

[32] Lapeña D, Lomba L, Artal M, Lafuente C, Giner B. The NADES glyceline as a potential green Solvent: A comprehensive study of its thermophysical properties and effect of water inclusion. *J Chem Thermodyn.* 2019; 128: 164-172. https://doi.org/10.1016/j.jct.2018.07.031

[33] Bahadori L, Chakrabarti MH, Mjalli FS, AlNashef IM, Manan NSA, Hashim MA. Physicochemical properties of ammonium-based deep eutectic solvents and their electrochemical evaluation using organometallic reference redox systems. *Electrochim Acta,* 2013; 113: 205-211. https://doi.org/10.1016/j.electacta.2013.09.102

[34] Troter DZ, Zlatković MZ, Đokić-Stojanović DR, Konstantinović SS, Todorović ZB. Citric acid-based deep eutectic solvents: Physical properties and their use as cosolvents in sulphuric acid-catalysed ethanolysis of oleic acid. *Adv Technol.* 2016; 5: 53-65. https://doi.org/10.5937/savteh1601053t

[35] Glasser L. Thermodynamic estimation: Ionic materials. *J Solid State Chem*. 2013; 206: 139-144. https://doi.org/10.15744/2348-9812.1.e105

[36] Haynes WM. CRC Handbook of chemistry and physics, A ready reference book of chemical and physical data, 94th ed., CRC Press, Taylor & Francis Group, Boca Raton, FL; 2013; pp. 12-21.

[37] Hayyan A, Mjalli FS, AlNashef IM, Al-Wahaibi YM, Al-Wahaibi T, Hashim MA. Glucose-based deep eutectic solvents: Physical properties. *J Mol Liq.* 2013; 178: 137. https://doi.org/10.1016/j.molliq.2012.11.025

[38] Born M, Wolf E. Principles of optics: electromagnetic theory of propagation, interference and diffraction of light, 7th Expanded Edition, Cambridge University Press, United Kingdom; 1999; pp. 11-14.

[39] Ghaedi H, Ayoub M, Sufian S, Shariff AM, Lal B, Wilfred CD. Density and refractive index measurements of transition-temperature mixture (deep eutectic analogues) based on potassium carbonate with dual hydrogen bond donors for CO_2 capture. *J Chem Thermodyn.* 2018; 118: 147. https://doi.org/10.1016/j.jct.2017.11.008

[40] Wu TY, Su S-G, Lin YC, Wang HP, Lin MW, Gung ST, Sun IW. Electrochemical and physicochemical properties of cyclic amine-based Brønsted acidic ionic liquids. *Electrochim Acta.* 2010; 56: 853-862. https://doi.org/10.1016/j.electacta.2010.09.084

[41] Đorđević BS, Troter DZ, Veljković VB, Kijevčanin MLj, Radović IR, Todorović ZB. The physicochemical properties of the deep eutectic solvents with triethanolamine as a major component. *J Serb Chem Soc.* 2020; 85: 1303-1315. https://doi.org/10.2298/JSC200425050D

[42] Esipovich A, Danov S, Belousov A, Rogozhin A. Improving methods of CaO transesterification activity. *J Mol Catal A Chem.* 2014; 395: 225-233. https://doi.org/10.1016/j.molcata.2014.08.011

[43] Veličković AV, Avramović JM, Stamenković OS, Veljković VB. Kinetics of the sunflower oil ethanolysis using CaO as catalyst. *Chem Ind Chem Eng Q.* 2016; 22: 409-418. https://doi.org/10.2298/ciceq160106003v
[44] Huang W, Tang S., Zhao H, Tian S. Activation of commercial CaO for biodiesel production from rapeseed oil using a novel deep eutectic solvent. *Ind Eng Chem Res.* 2013; 52: 11943-11947. https://doi.org/10.1021/ie401292w
[45] Manurung R, Ramadhani DA, Maisarah S. One step transesterification process of sludge palm oil (SPO) by using deep eutectic solvent (DES) in biodiesel production. *AIP Conf. Proc.* 2017; 1855: 070004. https://doi.org/10.1063/1.4985531
[46] Manurung R, Winarta A, Taslim Indra L. Biodiesel production from ethanolysis of palm oil using deep eutectic solvent (DES) as cosolvent, *IOP Conf. Ser.: Mater. Sci. Eng.* 2017; 206: 012023. https://doi.org/10.1088/1757-899X/206/1/012023
[47] di Bitonto L, Reynel-Avila HE, Mendoza-Castillo DI, Bonilla-Petriciolet A, Duran-Valle CJ, Pastore C. Synthesis and characterization of nanostructured calcium oxides supported onto biochar and their application as catalysts for biodiesel production. *Renew Energy.* 2020; 160: 52-66. https://doi.org/10.1016/j.renene.2020.06.045
[48] Chen X, Li Z, Chun Y, Yang F, Xu H, Wu X. Effect of the formation of diglycerides/monoglycerides on the kinetic curve in oil transesterification with methanol catalyzed by calcium oxide. *ACS Omega*. 2020; 5: 4646−4656. https://doi.org/10.1021/acsomega.9b04431
[49] Ramos M, Dias A PS, Teodoro F. Soybean oil ethanolysis over Ca based catalyst. Statistical optimization of reaction conditions. *React Kinet Mech Catal.* 2020; 130: 433-445. https://doi.org/10.1007/s11144-020-01791-y
[50] Sánchez-Cantú M, Reyes-Cruz FM, Rubio-Rosas E, Pérez-Díaz LM, Ramírez E, Valente JS. Direct synthesis of calcium diglyceroxide from hydrated lime and glycerol and its evaluation in the transesterification reaction. *Fuel*. 2014; 138: 126-133. https://doi.org/10.1016/j.fuel.2014.08.006
[51] Kouzu M, Hidaka J, Wakabayashi K, Tsunomori M. Solid base catalysis of calcium glyceroxide for a reaction to convert vegetable oil into its methyl esters. *Appl Catal A: Gen.* 2010; 390: 11-18. https://doi.org/10.1016/j.apcata.2010.09.029
[52] Rodriguez-Navarro C, Vettori I, Ruiz-Agudo E. Kinetics and mechanism of calcium hydroxide conversion into calcium alkoxides: implications in heritage conservation using nanolimes. *Langmuir*. 2016; 32: 5183-5194. https://doi.org/10.1021/acs.langmuir.6b01065
[53] Soares Dias AP, Ramos M, Catarino M, Puna J, Gomes J. Solvent assisted biodiesel production by co-processing beef tallow and soybean oil over calcium catalysts. *Waste Biomass Valorization*. 2019; 11: 6249-6259. https://doi.org/10.1007/s12649-019-00903-7

Uticaj temperature na fizičkohemijska svojstva eutektičkih rastvarača sa lecitinom i njihova upotreba u transesterifikaciji katalizovanoj CaO

Zoran B. Todorović[1], Biljana S. Đorđević[1], Dragan Z. Troter[1], Ljiljana M. Veselinović[2], Miodrag V. Zdujić[2] i Vlada B. Veljković[1,3]

[1]Tehnološki fakultet, Univerzitet u Nišu, Bulevar Oslobođenja 124, 16000 Leskovac, Srbija
[2]Institut tehničkih nauka Srpske akademije nauke i umetnosti, Knez Mihajlova 35, 11000 Beograd, Srbija
[3]Srpska akademija nauka i umetnosti, Knez Mihajlova 35, 11000 Beograd, Srbija

(Naučni rad)

Izvod

Zbog različitih strukturnih varijacija i mogućnosti prilagođavanja njihovih fizičkohemijskih svojstava, eutektički rastvarači se nazivaju ,,dizajnerski rastvarači". Za industrijsku primenu eutektičkih rastvarača, važno je poznavati njihova fizička i termodinamička svojstva poput gustine, viskoziteta i indeksa prelamanja. Ova svojstva su merena u funkciji temperature za tri eutektička rastvarača lecitina sa glicerolom, trietanolaminom i oleinskom kiselinom. Za opisivanje viskoziteta primenjene su Arenijusova i jednačina Vogela, Tamana i Fulčera (Vogel-Tamman-Fulcher). Gustina, viskozitet i indeks prelamanja testiranih eutektičkih rastvarača opadali su sa porastom temperature. Eutektički rastvarač lecitin:glicerol (LEC:G) je imao najmanju gustinu na svim testiranim temperaturama. Na kraju, eutektički rastvarač LEC:G je izabran kao kosolvent u etanolizi hladno ceđenog ulja semena crne slačice (*Brassica nigra* L.) katalizovanoj žarenim ili nežarenim CaO. Reakcija je izvedena u šaržnom reaktoru uz stalno mešanje i pri sledećim reakcionim uslovima: temperatura 70 °C, molski odnos etanol-ulje 12:1, koncentracija eutektičkog rastvarača 20 mas. % (u odnosu na masu ulja) i koncentracija CaO 10 mas. % (u odnosu na masu ulja). Prisustvo eutektičkog rastvarača ubrzalo je reakciju i separaciju faza finalne reakcione smeše..

Ključne reči: Brassica nigra L.; crna slačica; etanoliza; etil-estri masnih kiselina; eutektički rastvarači